ISSN 0006-2979, Biochemistry (Moscow), 2024, Vol. 89, No. 2, pp. 279-298 © Pleiades Publishing, Ltd., 2024.

Enhanced ROS Production in Mitochondria from Prematurely Aging mtDNA Mutator Mice

Irina G. Shabalina[1,a], Daniel Edgar[1,b], Natalia Gibanova[1,c], Anastasia V. Kalinovich[1,d], Natasa Petrovic[1,e], Mikhail Yu. Vyssokikh[1,f], Barbara Cannon[1,g], and Jan Nedergaard[1,h]*

[1]*Department of Molecular Biosciences, The Wenner-Gren Institute, Stockholm University, Stockholm, SE-106 91 Sweden*

[a]*e-mail: irina.shabalina@su.se* [b]*e-mail: the_daniel_edgar@hotmail.com* [c]*e-mail: ngibanova@gmail.com*

[d]*e-mail: anastasia@atrogi.com* [e]*e-mail: Natasa.Petrovic@su.se* [f]*e-mail: mikhail.vyssokikh@gmail.com*

[g]*e-mail: barbara.cannon@su.se* [h]*e-mail: jan.nedergaard@su.se*

Received November 17, 2023
Revised January 20, 2024
Accepted January 21, 2024

Abstract—An increase in mitochondrial DNA (mtDNA) mutations and an ensuing increase in mitochondrial reactive oxygen species (ROS) production have been suggested to be a cause of the aging process ("the mitochondrial hypothesis of aging"). In agreement with this, mtDNA-mutator mice accumulate a large amount of mtDNA mutations, giving rise to defective mitochondria and an accelerated aging phenotype. However, incongruously, the rates of ROS production in mtDNA mutator mitochondria have generally earlier been reported to be lower – not higher – than in wildtype, thus apparently invalidating the "mitochondrial hypothesis of aging". We have here re-examined ROS production rates in mtDNA-mutator mice mitochondria. Using traditional conditions for measuring ROS (succinate in the absence of rotenone), we indeed found lower ROS in the mtDNA-mutator mitochondria compared to wildtype. This ROS mainly results from reverse electron flow driven by the membrane potential, but the membrane potential reached in the isolated mtDNA-mutator mitochondria was 33 mV lower than that in wildtype mitochondria, due to the feedback inhibition of succinate oxidation by oxaloacetate, and to a lower oxidative capacity in the mtDNA-mutator mice, explaining the lower ROS production. In contrast, in normal forward electron flow systems (pyruvate (or glutamate) + malate or palmitoyl-CoA + carnitine), mitochondrial ROS production was higher in the mtDNA-mutator mitochondria. Particularly, even during active oxidative phosphorylation (as would be ongoing physiologically), higher ROS rates were seen in the mtDNA-mutator mitochondria than in wildtype. Thus, when examined under physiological conditions, mitochondrial ROS production rates are indeed increased in mtDNA-mutator mitochondria. While this does not prove the validity of the mitochondrial hypothesis of aging, it may no longer be said to be negated in this respect. This paper is dedicated to the memory of Professor Vladimir P. Skulachev.

DOI: 10.1134/S0006297924020081

Keywords: mtDNA mutator mice, ROS production, aging, succinate, membrane potential, oxidative phosphorylation

INTRODUCTION

Aging has been suggested to be a consequence of accumulation of mutations of mitochondrial DNA (reviewed in [1]). According to this, "*the mitochondrial hypothesis of aging*", these mutations would lead to errors occurring in the proteins of the respiratory chain, which in turn would lead to increases in mitochondrial production of reactive oxygen species (ROS). The ROS generated in this way would then lead to oxidative damage of cellular proteins, DNA, and lipids, which would finally manifest as aging [2, 3]. There is, however, presently no agreement concerning the validity of this hypothesis [4-6].

Abbreviations: mtDNA, mitochondrial DNA; ROS, reactive oxygen species.

* To whom correspondence should be addressed.

A substantial number of studies do support a role for mtDNA mutations in aging (reviewed in [7, 8]). There are several studies showing increased ROS production with age in both animal systems and humans [9-13]. However, not all studies agree [14, 15]). In reality, the generally observed parallel increase of ROS and mtDNA mutations with age has made it difficult to determine a cause-and-effect relationship [16, 17].

In this conundrum, the construction of the mtDNA mutator mouse [18, 19] should principally enable separation of cause and effect. Indeed, solely due to an increased rate of mitochondrial DNA mutations, this mouse shows features that can adequately be described as signs of premature aging, and it also has a significantly reduced lifespan [18, 19]. Whether this is a model that replicates the normal aging process may be discussed [1]. However, it undoubtedly opens for studies of the processes that lead from mitochondrial DNA mutations to the features of premature aging. Studies of this mouse should then be a way of establishing the possible significance of ROS production for aging.

Thus, in the mitochondrial hypothesis of aging, a predicted feature of increased mtDNA mutations would be an increased level of ROS. This ROS would then be responsible for the protein alterations that finally manifest themselves in features of premature aging. However, contrary to such expectations, in the mitochondrial mutator model, there is little evidence of oxidative damage [20-22]. Additionally and importantly, when the mutator mitochondria have been analyzed *ex vivo*, no increase in production of ROS by isolated mitochondria has been reported [23, 24], severely weakening the mitochondrial oxidative damage theory of aging [5].

However, despite these observations, certain *in vivo* investigations imply that an increased level of ROS production is involved in the aging process observed in the mtDNA mutator mice. For example, we have used the mitochondria-targeted mass spectrometry probe MitoB for estimation of hydrogen peroxide within mitochondria of living mice. In these studies, the *in vivo* level of mitochondrial hydrogen peroxide was enhanced in old mtDNA mutator mice, suggesting that the prolonged presence of mtDNA mutations *in vivo* increases hydrogen peroxide production that could contribute to an accelerated aging phenotype [25]. Additionally, when the mtDNA mutator mice were treated with the mitochondrially targeted antioxidant SkQ that would reduce ROS levels, the aging process of the mtDNA mutator mice was markedly delayed [26]. Similarly, in mice overexpressing catalase targeted to mitochondria, heart hypertrophy and fibrosis in the mtDNA mutator mice was attenuated [27]. These *in vivo* observations are thus supportive for an increase in ROS being the cause of the aging process and for this increase being an effect of the mitochondrial mutations. The reason for the apparent discrepancy of the results obtained *ex vivo* and *in vivo* is currently unknown.

In the present study, we have therefore re-examined ROS production in mitochondria isolated from heart and liver of the mtDNA mutator mice. In particular, we have focused on examining the mitochondria when they are metabolizing physiologically relevant substrates and doing this during active oxidative phosphorylation, i.e., we have examined conditions that may be said to more closely reflect the situation *in vivo*. We conclude that under these more physiologically relevant conditions, the mitochondria from the mtDNA mutator mice do produce more ROS, and the mitochondrial hypothesis for aging is thus not negated in this respect.

MATERIALS AND METHODS

Animals. Mice heterozygous for the mtDNA mutator allele (*+/PolgA^{mut}*) [18] were backcrossed to C57Bl/6 mice for at least 6 generations. After intercrossing mice heterozygous for the *PolgA^{mut}* allele and genotyping the offspring as previously described [18], *mtDNA mutator* mice were identified as the homozygote transgenic offspring; heterozygote offspring were not used; homozygote wildtype offspring were used as *wild-type* mice. The mice were fed *ad libitum* (R70 Standard Diet, Lactamin), had free access to water, and were kept on a 12 : 12 h light : dark cycle in cages with 4-5 animals at 24°C. The animals were routinely examined at the age of 25 weeks, i.e., at a time point where the first symptoms of premature aging, e.g. slight kyphosis, alopecia, and impaired weight gain, are observable in the mtDNA mutator mice [18, 26]. Oxidative stress biomarkers were measured in mice at the age of 40 weeks, i.e., at a time where symptoms of aging become grossly evident [26]. Animal protocols were in accordance with guidelines for humane treatment of animals and were reviewed and approved by the Animal Ethics Committee of the North Stockholm region.

Tissue collection and mitochondrial isolation. Mice were anaesthetized for 1 min by a mixture of 79% CO_2 and 21% O_2 and decapitated. All experiments were made in parallel, i.e., preparations from wildtype and mtDNA mutator mice were directly compared on each experimental day. Hearts from two mice were placed into ice-cold medium containing 100 mM sucrose, 50 mM KCl, 20 mM K-TES, 1 mM EDTA and 0.1% (w/v) fatty-acid-free bovine serum albumin (BSA) and were freed of white fat and connective tissue, weighed and used for mitochondrial isolation. Liver mitochondria were isolated as previously described [28, 29].

The tissues were finely minced with scissors and homogenized in a Potter homogenizer with a Teflon pestle.

During mincing and homogenizing, the heart fragments were treated with nagarse, added to the medium at a concentration of 1 mg per g of tissue. Throughout the isolation process, tissues were kept at 0-2°C.

Mitochondria were isolated by differential centrifugation. Tissue homogenates were centrifuged at 8500*g* for 10 min at 2°C using a Beckman J2-21M centrifuge. The resulting supernatant, containing floating fat and nagarse, was discarded. The pellet was resuspended in ice-cold medium containing 100 mM sucrose, 50 mM KCl, 20 mM K-TES, 1 mM EDTA and 0.2% (w/v) fatty-acid-free BSA. The resuspended homogenate was centrifuged at 800*g* for 10 min, and the resulting supernatant was centrifuged at 8500*g* for 10 min. The resulting mitochondrial pellet was resuspended in the same buffer (but albumin-free) and centrifuged again at 8500*g* for 10 min. The final mitochondrial pellets were resuspended by hand homogenization in a small glass homogenizer in the same medium. The concentration of mitochondrial protein was measured using fluorescamine [30] with BSA as a standard. Mitochondrial suspensions were kept on ice for no longer than 4 h during measurements.

All mitochondrial preparations were tested by quality control traces, examining adequate respiratory control by following the effect of ADP and FCCP additions on Complex I substrate respiration rates.

Mitochondrial ROS net production in heart mitochondria. Mitochondrial H_2O_2 net production in heart mitochondria was determined fluorometrically by the use of the *Amplex Red™ reagent*, Trade Mark of Molecular Probes, USA. Oxidation of Amplex Red coupled through horseradish peroxidase to reduction of H_2O_2 produces the red fluorescent product resorufin [31]. Mitochondria (0.05-0.2 mg of mitochondrial protein ml^{-1}) were incubated at 37°C in a buffer consisting of 100 mM sucrose, 20 mM K^+-Tes (pH 7.2), 50 mM KCl, 2 mM $MgCl_2$, 1 mM EDTA, 4 mM KP_i and 0.1 % fatty-acid-free BSA. All incubations also contained 5 μM Amplex Red, 12 units ml^{-1} horseradish peroxidase and 45 units ml^{-1} superoxide dismutase. The reaction was routinely initiated by addition of mitochondria followed by the successive addition of substrate: Complex II substrate (5 mM succinate), or Complex I substrates (2 mM malate + 5 mM pyruvate for heart (2 mM malate + 5 mM glutamate for liver) or a fatty acid-derived substrate (30 μM palmitoyl-CoA + 5 mM carnitine), followed by successive addition of rotenone (1.7 μM), antimycin A (3 μg/ml) and myxothiazol (0.8 μM) or ADP (450 μM).

The fluorescent signal was measured by three techniques: (1) kinetics of fluorescence emitted through a band pass filter of 600 ± 20 nm from an excitation wavelength of 545 nm was followed in a 3 ml cuvette for 10-15 min (2 points per sec) with a SIGMA ZWS-11 spectrofluorometer (SIGMA instrument GMBH, Berlin, Germany); (2) simultaneous fluorescent signals from mitochondrial samples supported by various substrates and ADP were detected with an EnSpire Multimode Plate Reader (PerkinElmer, USA) in a 24-well plate. The excitation wavelength 563 nm and the emission wavelength 584 nm were set by applying the optimisation mode of EnSpire plate reader. (3) Simultaneous measurements of fluorescence and oxygen consumption rates were performed by the O2k-MultiSensor System (Oroboros Instruments Corp., Innsbruck, Austria).

The rate of H_2O_2 production was calculated as the change in fluorescence intensity during the linear increase, as earlier described [32]. Calibration curves were obtained by adding known amounts of freshly diluted H_2O_2 (concentration of stock solution was checked at 240 nm using a molar extinction coefficient of 43.6) to the assay medium. The standard curve was linear in a range up till 500 nM H_2O_2.

Mitochondrial ROS net production in liver mitochondria. The measurement of H_2O_2 production in *liver mitochondria* is problematic due to the presence of catalase in the mitochondria [33, 34]. Therefore, we measured superoxide for examination of ROS production in liver mitochondria. Superoxide was measured using the superoxide-induced conversion of dihydroethidium (DHE) (Molecular Probes) to ethidium at 37°C using an excitation wavelength of 495 nm and collecting the emission via a narrow band pass filter at 570 ± 5 nm with a SIGMA ZWS-11 spectrofluorometer (SIGMA instrument GMBH, Berlin, Germany) [29, 32]. For validation of DHE as a potent tool for ROS measurement, we have earlier compared the DHE and Amplex Red methods and obtained qualitatively similar results [32].

Mitochondrial oxygen consumption. Heart mitochondria (0.1-0.2 mg protein/ml) were incubated in a medium of the same composition as that used for ROS production. Oxygen consumption rates were monitored using two techniques: an O2k-MultiSensor System (Oroboros Instruments Corp. Innsbruck, Austria) and a Clark-type oxygen electrode (Yellow Springs Instrument Co., USA) in a sealed incubation chamber at 37°C, as earlier described [35]. The output signal from the Clark-type electrode amplifier was electronically time-differentiated and collected every 0.5 s by a PowerLab/AD Instrument (application program Chart v5.0.1.). Phosphorylation state 3 was measured in the presence of 450 μM ADP. State-4 respiration was measured as the residual respiration after addition of 2 μg/ml oligomycin. Maximal oxygen consumption rates (uncoupled state) were obtained by addition of FCCP at a final concentration of 1.0-1.4 μM.

Mitochondrial membrane potential. Mitochondrial membrane potential measurements were performed with the dye safranin O [36]. The changes in absorbance of safranin O were followed at 37°C in

an Olis® modernized Aminco DW-2 dual-wavelength spectrophotometer at 511-533 nm with a 3-nm slit. Olis GlobalWorks™ software was used for recording and quantification. Calibration curves were made for each mitochondrial preparation in K^+-free medium and were obtained from traces in which the extramitochondrial K^+ was altered by addition of KCl in a 0.1-20 mM final concentration range in the presence of 3 μM valinomycin. The change in absorbance caused by each addition was plotted against $[K^+]$out and the intramitochondrial K^+, $[K^+]$in, was estimated by extrapolation of the line to the zero-uptake point, as described [36]. The absorbance readings were used to calculate the membrane potential (mV) by the Nernst equation according to: $\Delta\psi = 61\ mV \cdot \log([K^+]in / [K^+]out)$.

Proton leak. To determine proton leak, mitochondrial membrane potential and oxygen consumption measurements were performed in parallel using the same media consisting of 100 mM sucrose, 20 mM K^+-Tes (pH 7.2), 50 mM KCl, 2 mM $MgCl_2$, 1 mM EDTA, 4 mM KPi, 0.1 % fatty-acid-free BSA, 2 μg/ml oligomycin, 5 μM safranin O and 5 mM succinate, in the presence of increasing amounts of malonate (0.5-3.3 mM), at 37°C. An energizing preincubation time of ≈3.5 min was used before malonate additions; proton leak kinetic measurements were finalized within 11-12 min as in [35].

Protein oxidative modification biomarkers. Oxidative stress biomarkers were analyzed in liver total tissue homogenate. For collection of tissue, mice were anaesthetized for 1-2 min by a mixture of 79% CO_2 and 21% O2 and decapitated. Tissues were dissected out and rapidly placed in liquid nitrogen; then tissues were powdered under liquid nitrogen, weighed, divided into small amounts and stored under nitrogen at –80°C. A small amount was homogenized in RIPA buffer with proteinase inhibitor (Complete Mini, Roche) and protein concentration measured.

4-HNE-adducts was detected by immunoblot analysis with polyclonal antibodies from Alpha Diagnostics (HNE12-S, dilution 1 : 1000) as described [37, 38]. 4-HNE-BSA protein conjugate (HNE12-C, Alpha Diagnostics) was used as an internal control.

Carbonyl groups of proteins were analysed by OxyBlot Protein oxidation detection kit (Chemicon International) consisting of several steps: derivatization of carbonyl groups to 2,4-dinitrophenylhydrazone (DNP-hydrazone), separation of protein samples by SDS PAGE (12%), and Western blotting using primary antibodies specific to the DNP moiety of the proteins. A mixture of Standard Proteins with attached DNP residues (Chemicon International) was used as internal control.

Statistics. KaleidaGrapH 4.5.2 Synergy Software (Reading, USA) was used for the graphs and statistical analysis. Groups were compared with Student's two-tailed *t*-test. All data were expressed as means ± SE. Significance was accepted at the level of $p < 0.05$ (indicated in the graphs by one symbol), $p < 0.01$ (two symbols) and $p < 0.001$ (three symbols).

RESULTS

To clarify the relationship between mitochondrial DNA mutations and ROS production, we examined ROS production in mitochondria isolated from heart and liver of the mtDNA mutator and wildtype mice. We utilized a series of protocols for examination of ROS production and clarified the cause for the differences seen. We finally examined whether the alterations in ROS production were associated with differences in degrees of oxidative damage.

Diminished ROS production in mitochondria from mtDNA mutator mice under classical ROS assessment conditions. ROS production in isolated mitochondria is classically examined with the complex II-coupled substrate succinate (reviewed in [39-41]). Besides being a classical *in vitro* approach to ROS measurement as such, succinate-supported ROS production has attracted much attention in the longevity field since it somewhat puzzlingly has been proposed as both being involved in lifespan reduction [42] and lifespan extension [43].

In isolated mitochondria, added succinate is oxidized by Complex II and this reduces ubiquinone (Q) and generates a proton-motive force that is sufficiently high to drive electrons thermodynamically uphill through Complex I, to reduce NAD^+ to NADH (reverse electron flow). This results in superoxide production from semi-reduced coenzyme Q (semiquinone) at the coenzyme Q-binding site of Complex I [44, 45]. We initially used this standard condition for ROS production to examine mitochondria isolated from the heart and liver of wildtype and mtDNA mutator mitochondria. H_2O_2 production from the heart was measured with the Amplex Red system as exemplified with a representative trace (Fig. 1a); for liver mitochondria, the DHE method was used (Fig. 1b) (see Materials and Methods section).

ROS from Complex I. After addition of succinate, wildtype mitochondria displayed a high amount of ROS production, which was markedly inhibited in heart mitochondria by rotenone (Fig. 1a). A similar effect was seen with liver mitochondria (Fig. 1b). Rotenone inhibits Complex I at subunit ND1 [46]. The inhibition by rotenone therefore indicated that Complex I was the major site of ROS production in these mitochondria, and that electrons required for ROS production are delivered to Complex I by reverse electron transport from Complex II.

There was a clearly diminished rate of ROS production in heart mitochondria from mtDNA mutator,

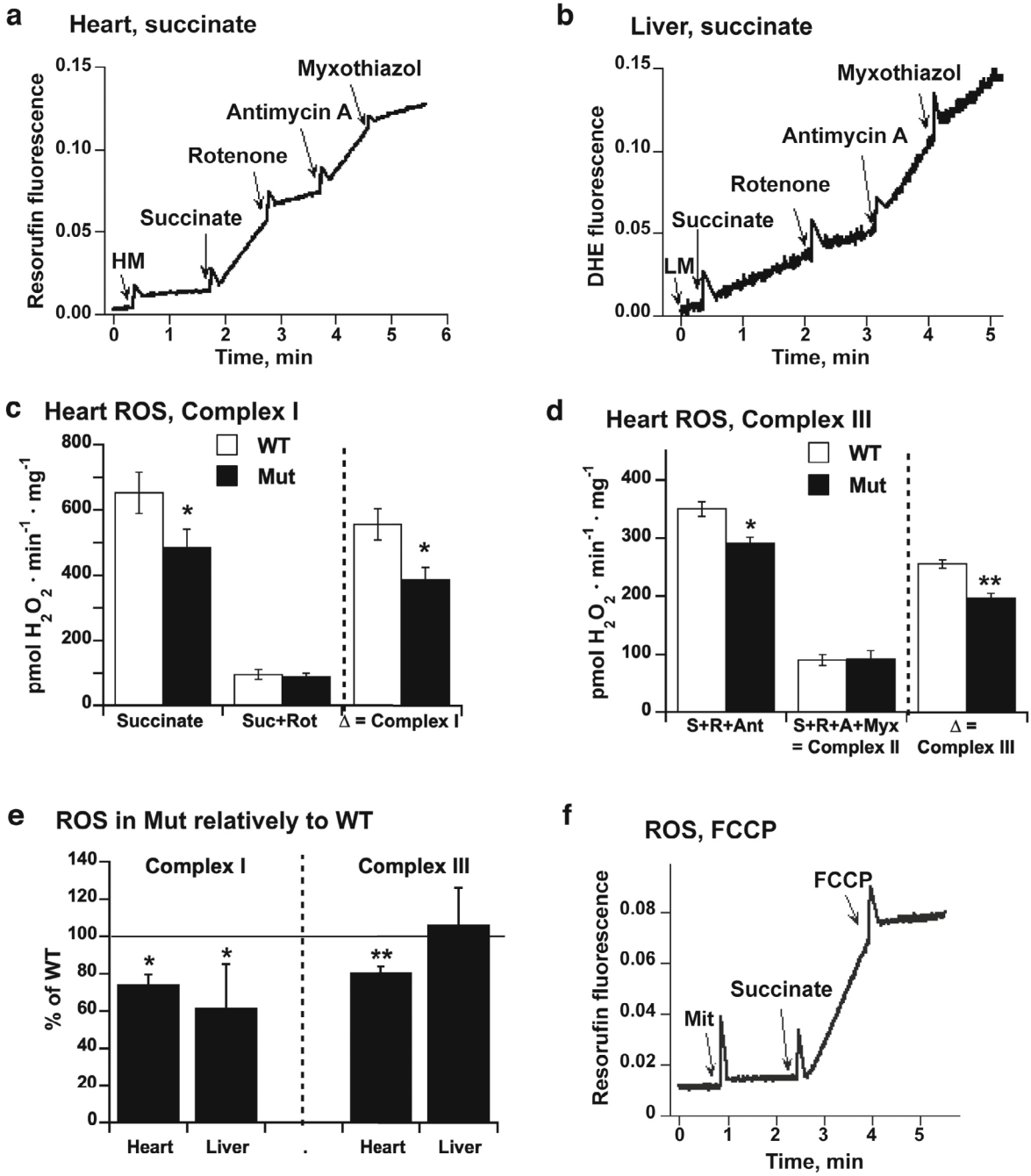

Fig. 1. ROS production in mitochondria energized by succinate and examined under traditional conditions. a, b) A representative trace of (a) Amplex Red fluorescence and (b) dihydroethidium (DHE) measurements in wildtype heart (a) and liver (b) mitochondria energized by succinate. Additions were 0.1 mg/ml heart (HM) or liver (LM) mitochondria, 5 mM succinate, 1.7 μM rotenone, 3 mg/ml antimycin A and 0.8 μM myxothiazol. c) Hydrogen peroxide production rate under conditions of reverse electron flow from Complex I (measured principally as shown in (a) and expressed as hydrogen peroxide amount, based on calibration) in heart mitochondria isolated from wildtype (WT, white bars) and mtDNA mutator mice (Mut, black bars). The difference between the rate with succinate alone and that after the further addition of rotenone (Δ) is considered to represent ROS production from Complex I. d) Hydrogen peroxide production rate after antimycin A addition (as in a) in heart mitochondria isolated from wildtype and mtDNA mutator mice, the rate after further myxothiazol addition, and the Δ between these. The rate after myxothiazol represents ROS from Complex II and the Δ rate ROS from Complex III. e) Relative ROS production rates from Complex I and Complex III in mitochondria isolated from mtDNA mutator mice. ROS refers to hydrogen peroxide in heart (measured as in a) and to the change in DHE fluorescence signal intensity in liver mitochondria (measured as in b). For each preparation day, the Δ (b) rate in wildtype mitochondria was set to as 100% and the Δ rate in mtDNA mutator was expressed as a percentage of this. Values in (c)-(e) represent means ± SE of 5-7 independent parallel mitochondrial preparations. *, ** Indicate statistically significant differences between wildtype and mtDNA mutator mice ($p < 0.05$, < 0.01). f) A representative trace of the effect of FCCP on Amplex red fluorescence (H_2O_2 levels) measured in wildtype heart mitochondria energized by succinate. Additions were 0.2 mg/ml mitochondria (Mit), 5 mM succinate, and 1.4 μM FCCP.

compared to that in wildtype mitochondria (Fig. 1c). The small amount of residual ROS generated in mitochondria after rotenone addition was not different between wildtype and mtDNA mutator mitochondria (Fig. 1c). We defined the Complex I-derived ROS as the difference (delta) in ROS production before and after addition of rotenone. ROS production from Complex I was thus clearly reduced in the heart mitochondria from the mtDNA mutator mice (Fig. 1c). Similarly to the case in heart mitochondria (Fig. 1c), liver mtDNA mutator mitochondria produced less ROS from Complex I than did wildtype mitochondria (Fig. 1e).

From Complex III. Another major site capable of producing ROS under these conditions is Complex III (forward electron flow from Complex II). To study this site, we further added first antimycin A and then myxothiazol to the mitochondria (Fig. 1, a, b). Antimycin A is a Complex III Q_i-site inhibitor that blocks electron transfer from b heme to quinone, resulting in increased formation of semiquinone at the Q_o-site of Complex III, which in turn can transfer an electron to oxygen, yielding superoxide. In heart and liver mitochondria, antimycin A addition accordingly increased ROS production (Fig. 1, a, b). Also, here, ROS production was lower in mtDNA mutator mitochondria (Fig. 1d). Myxothiazol blocks electron entry from Complex II into the Q_o-site of Complex III, preventing the formation of this semiquinone and hence decreasing ROS production (Fig. 1, a, b). Thus, after myxothiazol addition, ROS production from Complex III is blocked, and also reverse electron transport into Complex I is here blocked by rotenone (Fig. 1, a, b). We thus define Complex III-derived ROS production as the difference (delta) between the ROS production rate after antimycin A and after myxothiazol (Fig. 1d). Defined in this way, it is seen that ROS production from Complex III in mtDNA mutator mice was 18 % lower in heart mitochondria. The production in liver mitochondria was unchanged (Fig. 1e).

From Complex II. After myxothiazol addition (Fig. 1, a, b), the only residual ROS production should be from Complex II. This rate was equal in wildtype and mtDNA mutator mitochondria from heart (Fig. 1d), as well as from liver (not shown). Thus, the conclusion from these standard experiments with succinate as electron donor was that mtDNA mutator mitochondria showed either an unchanged (from Complex II) or a clearly diminished rate of ROS production (from Complexes I and III). It is thus obvious that the *in vitro* ROS measurements in succinate-supported mitochondria yield results that are in direct contrast to the results obtained in *in vivo* measurements [25].

The low membrane potential in the mtDNA mutator mitochondria respiring on succinate may explain the low ROS production rate. In order to obtain further insight into the physiological relevance of the use of succinate for studying ROS production in mitochondria *in vitro*, we analyzed the bioenergetics of mitochondria under the conditions classically used for measuring ROS production. In particular we focused on how ROS produced through succinate-supported respiration is dependent on the membrane potential.

ROS production in mitochondria energized by succinate-induced reverse electron flow is susceptible to changes in the membrane potential (reviewed in [39-41] and seen by us in brown adipose tissue mitochondria [32]). Indeed, the uncoupler FCCP eliminates the high ROS production supported by reverse electron transport in heart mitochondria (Fig. 1f), as expected [47, 48]. Thus, the observed low ROS production in mtDNA mutator mitochondria oxidizing succinate (Fig. 1) could be due to a lower membrane potential in the mitochondria isolated from these mice.

We assessed the membrane potential by safranin O absorbance in mitochondria respiring on succinate without rotenone (Fig. 2). The membrane potential was stable for both wildtype and mtDNA mutator mitochondria (Fig. 2a). It was eliminated by FCCP (Fig. 2a). After calibration of each mitochondrial preparation versus K^+ gradients, we calculated the membrane potential to be as much as 33 mV lower in mtDNA mutator mitochondria than in wildtype mitochondria (200 mV wildtype vs 167 mV mutant) (Fig. 2b), suggesting that a low membrane potential could be the reason for the reduction in ROS production seen in the mtDNA mutator mitochondria under these conditions: the energy may not be enough to support the reverse electron flow to Complex I.

To establish the cause of the lower membrane potential, we first examined the respiratory capacity of heart mitochondria under these conditions. As seen in Fig. 2c, contrary to what is expected in isolated mitochondria the respiration rate of wildtype heart mitochondria was not limited by proton leak: addition of the uncoupler FCCP induced just a brief increase in respiration with subsequent inhibition, principally in agreement with e.g., [49]. Also, in the mtDNA mutator mitochondria, the respiration was not regulated by the membrane potential, as FCCP addition also here led to inhibition of respiration (Fig. 2c) after a short stimulation.

However, when mitochondria respire on succinate in the absence of rotenone (as is the case in the classical design for studying ROS production used here), there may be an inhibition of Complex II (succinate dehydrogenase) activity due to the successive accumulation of oxaloacetate in the mitochondria; this oxaloacetate will with high affinity compete with succinate for the binding site in Complex II [50]. Thus, this inhibition may limit the rate of succinate oxidation and the oxidative rate is then not regulated by proton leak through the membrane.

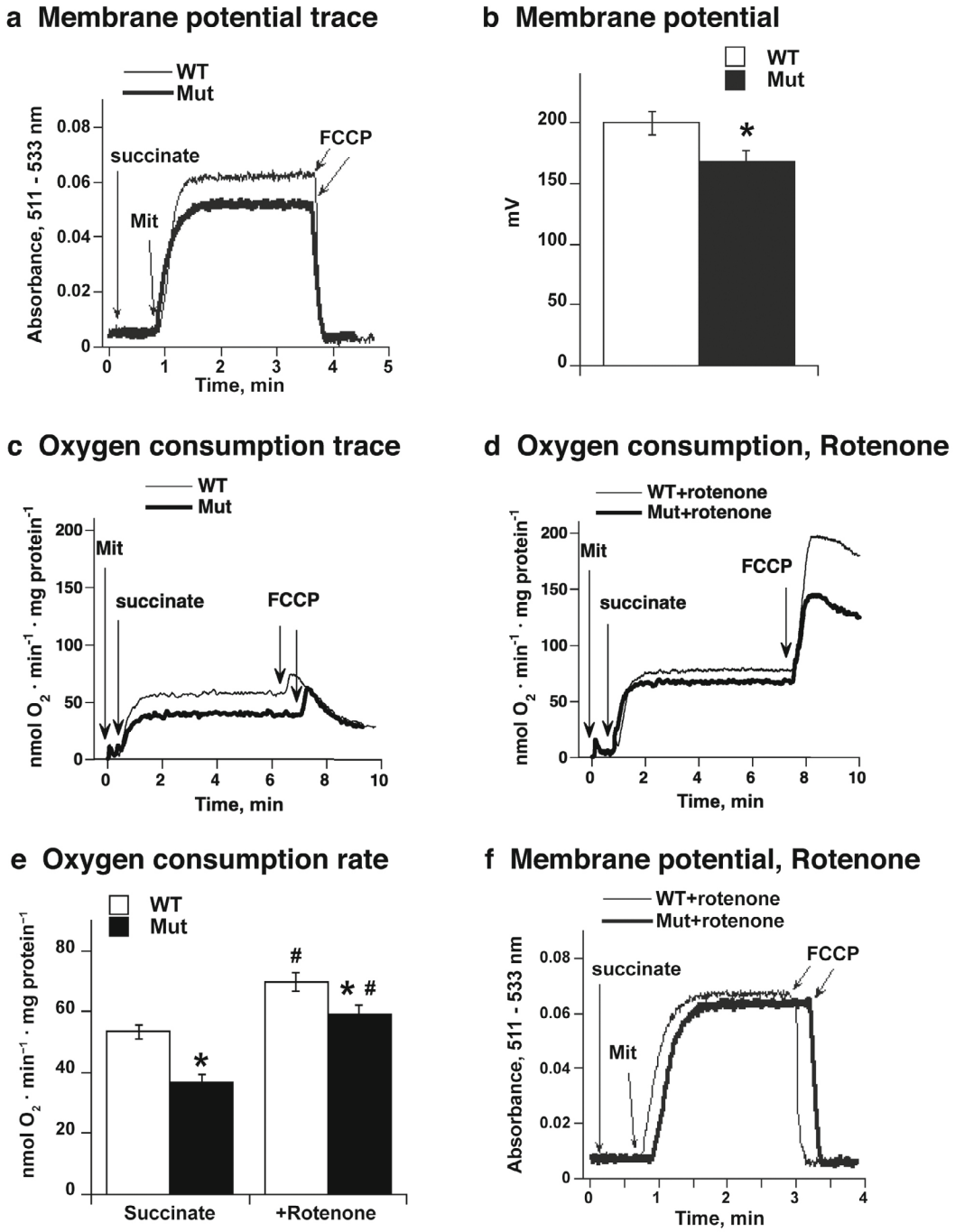

Fig. 2. The effect of rotenone on succinate-supported respiration and membrane potential. a) Representative traces of membrane potential measurements in heart mitochondria isolated from wildtype (*thin line*) and mtDNA mutator mice (*thick line*). Additions were 5 mM succinate, 0.2 mg/ml mitochondria (*Mit*), and 1.4 μM FCCP. b) Comparison of membrane potential levels in heart mitochondria from wildtype and mtDNA mutator mice, examined principally as in (a). Values represent means ± SE of 6 independent parallel mitochondrial preparations. * Indicates statistically significant difference between wildtype and mtDNA mutator mice ($p < 0.05$). c) Respiratory traces comparing succinate-supported respiration of wildtype (*thin line*) and mtDNA mutator (*thick line)* heart mitochondria in the absence of rotenone. Additions were as in (a). d) Respiratory traces comparing succinate-supported respiration of wildtype (*thin line*) and mtDNA mutator (*thick line)* heart mitochondria in the presence of rotenone (1.7 μM). Additions were 0.2 mg mitochondria (*Mit*), 5 mM succinate, 2 μg/ml oligomycin, and 1.4 μM FCCP. e) The effect of rotenone on succinate-supported oxygen consumption rate in heart mitochondria from wildtype and mtDNA mutator mice, examined principally as in (c) and (d), rate after succinate addition. Values represent means ± SE of 4-6 independent parallel mitochondrial preparations. * Indicates statistically significant difference between wildtype and mtDNA mutator mice ($p < 0.05$) and # indicates significant effect of rotenone ($p < 0.05$). f) Absorbance traces comparing succinate-supported membrane potential of wildtype (*thin line*) and mtDNA mutator (*thick line)* heart mitochondria in the presence of rotenone (1.7 μM). Additions as in (a). For direct comparisons, traces shown in a, c, d and f are from one experimental day, with parallel preparations of wildtype and mtDNA mutator mitochondria, examined in parallel for respiration and membrane potential.

Proton leak. To establish whether the lower membrane potential observed above in the mtDNA mutator mitochondria was due to respiratory limitation, rather than to increased proton leak (uncoupling), we made proton leak determinations. We examined proton leak kinetics under conditions where the mitochondria respired on succinate and oxygen consumption was successively inhibited with malonate, while assessing the membrane potential that could be reached when the capacity for succinate oxidation was thus successively (further) diminished.

The separate data on oxygen consumption and membrane potential were in themselves illustrative. Resting oxygen consumption rates were much lower in the mtDNA mutator mitochondria compared to wildtype (Fig. 3a), and the respiration in both types of mitochondria was inhibited by the first addition of malonate. As is evident from the data above, the membrane potential was markedly lower in mtDNA mutator mitochondria, but in contrast to respiration, the first addition(s) of malonate did not affect the membrane potential in a measurable way (Fig. 3b).

When these data were re-graphed as proton leak curves ("Brand plots"), i.e., as respiration as a function of the driving force (membrane potential), remarkable curve shapes resulted (Fig. 3c). At low membrane potentials (<170 mV), the respiration was very low but still may be said to be ohmic in that it was roughly proportional to the membrane potential. The curves for wildtype and mutator mitochondria are also nearly identical in this range, demonstrating that the increased mutation rate has not influenced the proton leak. However, at the higher membrane potentials, the rate of oxidation was no longer under the control of the membrane potential: only the (apparent) concentration of substrate (i.e., succinate still not inhibited by malonate) determined the rate of respiration. Such steep curves for succinate oxidation versus membrane potential have earlier been observed in other systems (liver mitochondria [51]) and similarly for glycerol-3-phosphate oxidation in brown adipose tissue mitochondria [52]. It is possible that our preparation contained small amounts of mitochondrial membrane fragments that may oxidize succinate unhampered by the mitochondrial membrane potential; matrix-free oxidation of succinate should be possible, as no soluble electron carriers (NAD^+) are needed for succinate (or glycerol-3-phosphate) oxidation.

In the mtDNA mutator mitochondria, the apparent breakpoint is decreased by as much as 32 mV, from ≈206 mV to ≈174 mV (Fig. 3c). This membrane potential is apparently the highest that can be reached in these mitochondria when the respiratory capacity is limited. Thus, the lower level of membrane potential is not associated with high membrane proton leak but instead reflects a diminished capacity for electron flux, and

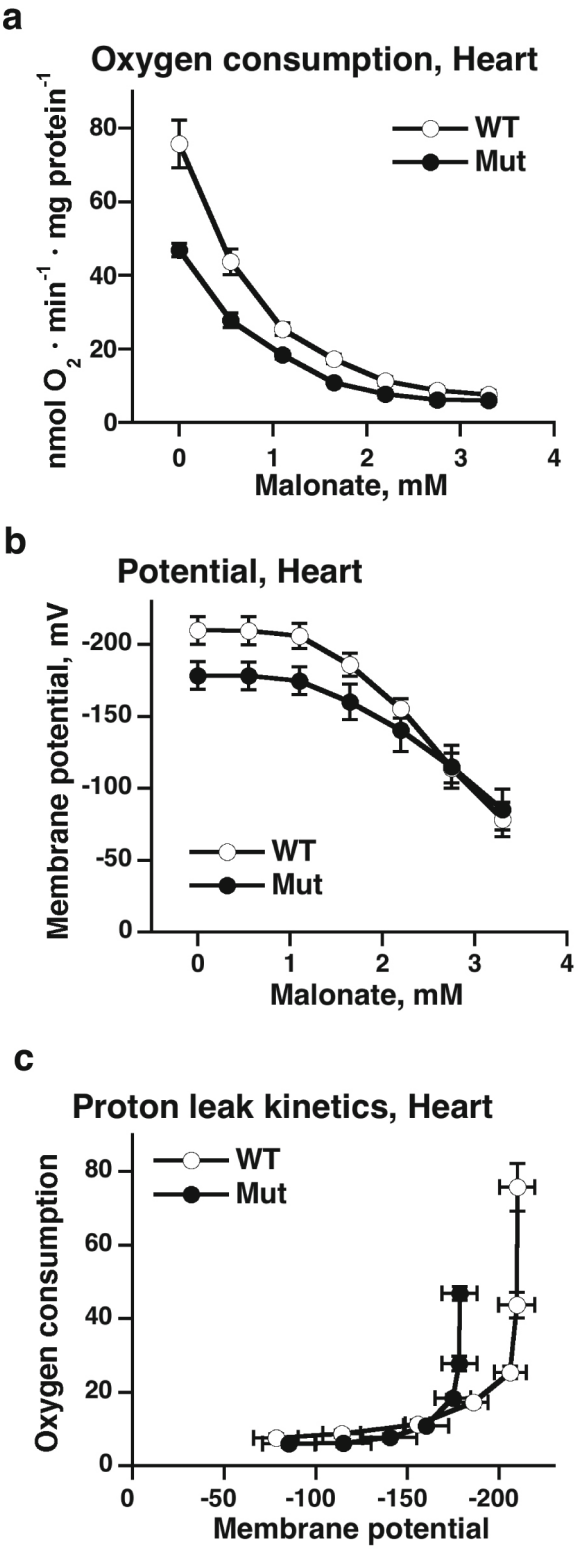

Fig. 3. Proton leak analysis in wildtype and mtDNA mutator mitochondria. Heart mitochondria were incubated principally as in Fig. 1, with succinate (in the absence of rotenone) as substrate, and oxygen consumption and membrane potential were determined in parallel under identical conditions, after addition of the indicated amounts of malonate. a) Oxygen consumption. b) Membrane potential. c) Proton leak kinetics based on the data in (a) and (b). The points are means ± SE from 7 independent mitochondrial preparations for each group.

the lowered membrane potential would explain why ROS production is lower on reverse electron transport in mtDNA mutator mitochondria.

The effect of rotenone. The inhibition of succinate respiration observed above is thus due to endogenously generated oxaloacetate. The accumulation of oxaloacetate should be eliminated by the addition of rotenone. Indeed, in the presence of rotenone, the respiration rate became sensitive to the membrane potential, as the addition of FCCP now led to a marked increase in respiratory rate (Fig. 2d) in the same mitochondrial preparation. The succinate-supported respiratory rate (state 4) increased in both wildtype and mtDNA mutator mitochondria in the presence of rotenone (Fig. 2e). The addition of rotenone also almost eliminated the difference in the levels of membrane potential between wildtype and mtDNA mutator mitochondria (Fig. 2f) (the membrane potentials calculated were now 207 mV versus 199 mV, i.e. the difference became only 8 mV).

Thus, we show here that mitochondria examined under the conditions (succinate as substrate without rotenone) widely used for studying the role of ROS in longevity [42, 43] are in a bioenergetically unusual state: the mitochondria are not in state 4, but a state where respiratory capacity and membrane potential are unphysiologically lowered, likely due to the accumulation of oxaloacetate in the mitochondria. The membrane potential that could be maintained in both types of mitochondria was thus unphysiologically low with the mtDNA mutator mitochondria only able to maintain an even lower potential (Fig. 2b), which probably explains the lower ROS production in these mitochondria (Fig. 1, a-c).

Obviously, under *in vivo* conditions, rotenone is not present, and it may thus be considered strange to claim that this condition, i.e., succinate plus rotenone, is more physiological than just succinate. However, to respire on only succinate is in itself unphysiological, and when the NADH from malate oxidation can be oxidized in Complex I, all oxidized succinate will give rise to oxaloacetate, a product that inhibits succinate dehydrogenase. Under physiological conditions, with fatty acids or glucose/pyruvate as substrate, the oxaloacetate will condense with incoming acetyl-CoA and thus not accumulate. Avoiding this accumulation by using rotenone is thus an experimental condition that – although it appears to be very artificial – more closely mimics physiological conditions better than the absence of rotenone.

Enhanced ROS production from mtDNA mutator mitochondria energized by Complex I substrates. Conditions such as those used above in the classical design of mitochondrial ROS experiments, i.e., external succinate respiration and accompanying backward electron flow, are rare *in vivo* [53-55]. We therefore continued by examining ROS production under other, more physiologically relevant, conditions. Physiologically, mitochondria are mainly energized with Complex I substrates and display forward electron flow. To examine these conditions, we allowed mitochondria isolated from heart or liver to respire on Complex I substrates, pyruvate + malate (Fig. 4a, shown for heart mitochondria with Amplex Red system) or glutamate + + malate (Fig. 4b, shown for liver mitochondria with DHE probe), and measured ROS production.

As seen (Fig. 4, a, b), the addition of substrate led to an immediate and linear rate of ROS production in both heart and liver mitochondria. When we compared the rate of ROS production between mitochondria from wildtype and mtDNA mutator mice, we found that, contrary to the case under classical reverse electron transport conditions (with succinate as substrate), mtDNA mutator mitochondria from both tissues investigated produced more ROS (heart 41% and liver 70%) than wildtype mitochondria (Fig. 4, c, d). Notably, oxygen consumption rates were not significantly diminished in the mutator mitochondria under these conditions [basal respiration (before FCCP)] (Fig. 4, e, f).

To identify the site of the increased ROS production, we added rotenone to the mitochondria. Since rotenone inhibits the flux of electrons from Complex I, all ROS must then originate from Complex I (or from upstream pyruvate or alpha-ketoglutarate dehydrogenases). The addition of rotenone increased ROS production in both wildtype and mtDNA mutator mitochondria (Fig. 4, a-d), as expected [12, 40, 41]. After rotenone addition, mtDNA mutator heart mitochondria still had greater ROS production than wildtype heart mitochondria, while liver mitochondria only showed a non-significant trend toward an increase (Fig. 4, c and d). This increased ROS production after rotenone addition may indicate that upstream systems, e.g., pyruvate dehydrogenase [56], could be an important site for ROS production in heart mitochondria, especially in the mtDNA mutator mice.

It is clear from Figs. 1 and 4 that the magnitude of ROS production observed with Complex I substrates compared to that observed with succinate is much lower; Complex I substrate gave less than 20% of the H_2O_2 production obtained from succinate. That a very high rate of ROS production is observed when succinate is used as the mitochondrial oxidative substrate probably explains why succinate is traditionally chosen when examining ROS production ([9, 37, 57]). However, it is clear that qualitatively remarkably different results were obtained when complex II and complex I substrates were analyzed, yielding contrasting conclusions concerning the significance of mitochondrial mutations for ROS production. Thus, it would seem that under conditions more resembling physiological

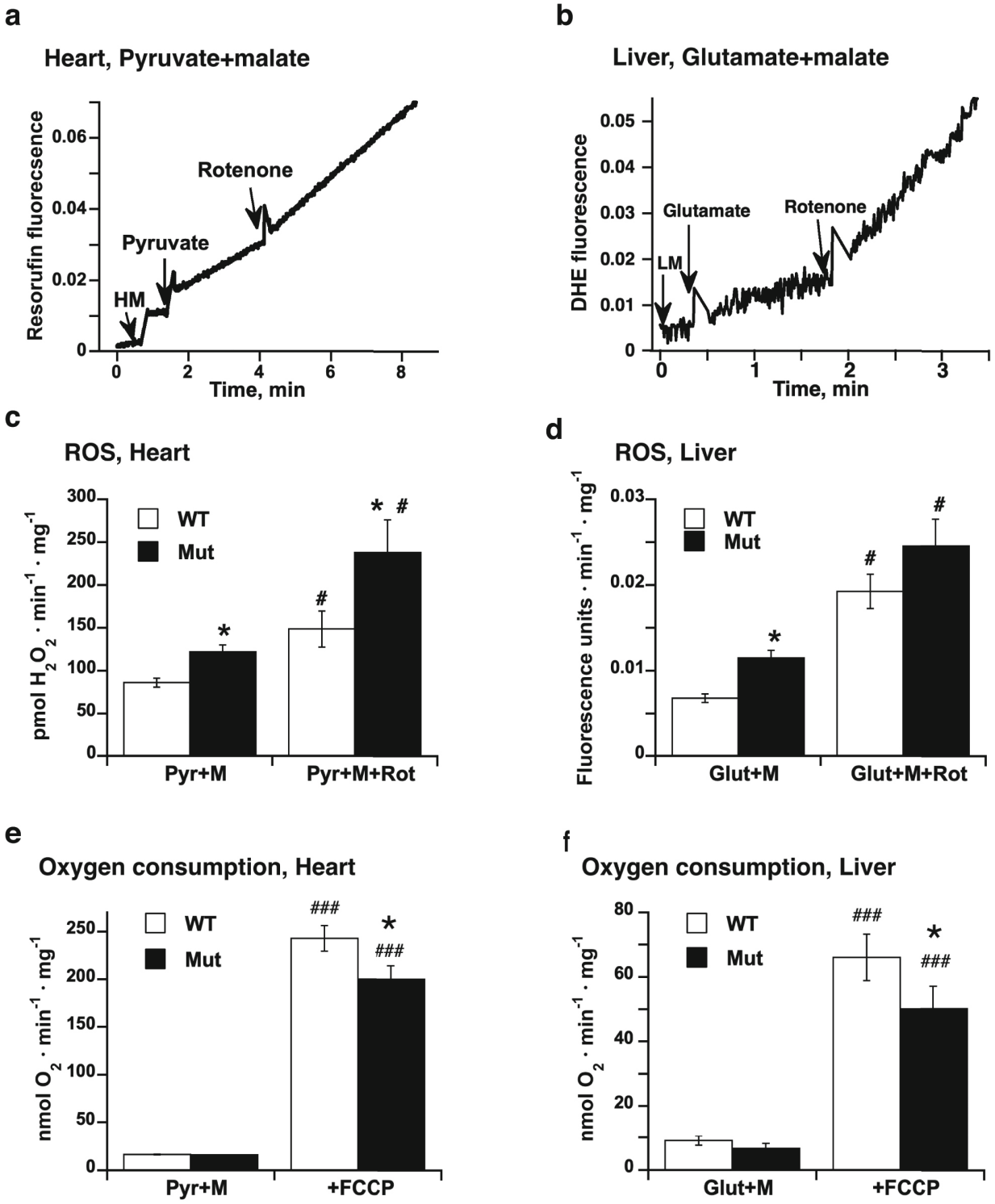

Fig. 4. ROS production in mitochondria energized by Complex I substrates. a, b) A representative trace of Amplex Red fluorescence (a) and dihydroethidium (DHE) (b) measured in wildtype heart (a) and liver (b) mitochondria energized by pyruvate + malate (a) or by glutamate + malate (b). Additions were 0.2 mg/ml heart (*HM*) or liver (*LM*) mitochondria, 5 mM pyruvate for heart mitochondria or 5 mM glutamate for liver mitochondria (2 mM malate was present in medium) and 1.7 μM rotenone. c, d) Rate of ROS production under conditions of forward electron flow supported by pyruvate + malate in heart (c) and glutamate + malate in liver (d) mitochondria (measured principally as in a and b). The values represent means ± SE of 4-9 independent mitochondrial preparations for each genotype. * Statistically significant difference between wildtype and mtDNA mutator mitochondria ($p < 0.05$); # statistically significant effect of rotenone ($p < 0.05$). e, f) Complex I substrate-supported oxygen consumption rates in heart and liver mitochondria from wildtype and mtDNA mutator mice. Values represent means ± SE of 4-9 independent parallel mitochondrial preparations. * Indicates statistically significant difference between wildtype and mtDNA mutator mice ($p < 0.05$). ### Indicates significant effects of FCCP ($p < 0.001$).

conditions, the mtDNA mutator mice do display a slightly higher – not a lower – ROS production rate than do wildtype mice.

Enhanced ROS production from mtDNA mutator mitochondria energized by fatty acid-derived substrates. In addition to pyruvate (and glutamate), fatty acids are physiologically relevant substrates for mitochondrial respiration, and the ROS production associated with fatty acid oxidation in the mtDNA mutator mice is therefore of physiological relevance. Similarly to what is the case for the classical Complex I substrates (pyruvate, glutamate), fatty acid oxidation occurs inside mitochondria and requires intact respiratory chain activity and ATP production [58].

In contrast to other substrates such as malate, glutamate, succinate or glycerol 3-phosphate, oxidation of fatty acids requires no less than four enzymatic reactions and donates electrons at several points in the electron transport chain: Complex I, ETFQOR, and Complex II (via formation of succinate in the Krebs cycle) [59]. Moreover, ROS production with fatty acid-derived substrates is evident across a physiological range of membrane potential and is relatively insensitive to membrane potential changes [32, 60]. This makes fatty acid oxidation a good candidate for high rates of superoxide or H_2O_2 formation, due to possible leaks of electrons to molecular oxygen at several different sites independently of membrane potential.

Therefore, we examined how mitochondrial ROS production with fatty acids as substrate is affected in the mtDNA mutator mice. The fatty acid-derived substrate palmitoyl-CoA, in the presence of carnitine, was a suitable substrate for heart wildtype mitochondria, providing a 10-fold increase in the rate of oxygen consumption after FCCP addition, i.e., the maximal oxidative capacity of heart mitochondria, exceeded the basal respiration rate ten times (Fig. 5a). Similar high oxidative capacity was observed in wildtype heart mitochondria supported by Complex I substrates (Fig. 4e), indicating that, for the heart, fatty acids are equally significant substrates as is glucose-derived pyruvate.

The rate of oxygen consumption in basal conditions (not stimulated by FCCP) was not different between wildtype and mtDNA mutator mitochondria supported by palmitoyl-CoA + carnitine (Fig. 5a), similarly to Complex I substrates (Fig. 4e), and in contrast to succinate where mutant mitochondria had a lower rate even in the basal state (Fig. 2e).

Both mtDNA mutator mitochondria supported by Complex I substrates or succinate had reduced spare oxidative capacity (the FCCP response) as compared to wildtype (Figs. 4e and 2d), in agreement with [28]. Surprisingly, high oxidative capacities supported by fatty acid-derived substrates were equal in wildtype and mutant mitochondria (Fig. 5a). Thus, oxidation of fatty acid substrates was not impaired, despite the severe

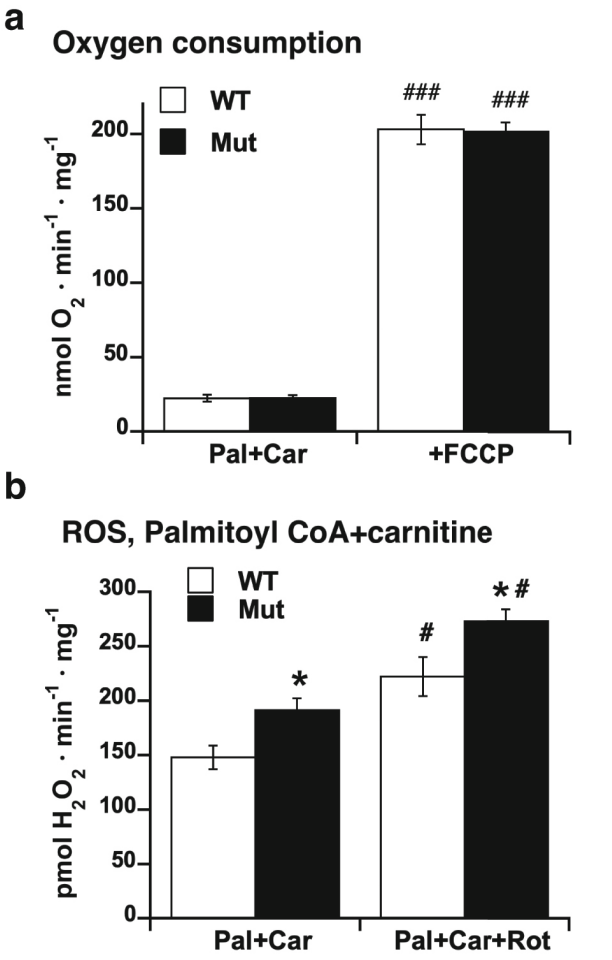

Fig. 5. ROS production in mitochondria energized by fatty acid-derived substrate (palmitoyl-CoA + carnitine). a) Basal and maximal (after FCCP) oxygen consumption supported by palmitoyl-CoA (30 μM) + carnitine (5 mM) in heart mitochondria from wildtype and mtDNA mutator mice. ### Indicates significant effects of FCCP ($p < 0.001$). b) Rate of ROS production supported by palmitoyl-CoA (30 μM) + carnitine (5 mM) in heart mitochondria from wildtype and mtDNA mutator mice, before and after addition of rotenone. * Statistically significant difference between wildtype and mtDNA mutator mitochondria ($p < 0.05$). # Indicates significant effects of rotenone ($p < 0.05$). In (a) and (b), the values represent means ± SE of 5 independent mitochondrial preparations for each genotype.

limitation in respiratory chain complexes in mtDNA mutator mice, in agreement with [23]. Therefore, it was interesting to see the high degree to which such substrates affected ROS production.

The rate of ROS production was 29% higher in mtDNA mutator heart mitochondria than in wildtype mitochondria when fatty acid-derived substrates were oxidized (Fig. 5b), similarly to what we observed with Complex I substrates (Fig. 4c) and in contrast to the reduced rate in the presence of succinate (Fig. 1c).

For fatty-acid derived substrates, the addition of rotenone increased ROS production in both wildtype and mtDNA mutator mitochondria from heart and the mtDNA mutator mitochondria had somewhat

higher ROS production than the wildtype mitochondria (Fig. 5b), similarly to what we observed with Complex I substrates (Fig. 4c).

Thus, *in vitro*, ROS measurement in mitochondria supported by Complex I and fatty acid-derived substrates yields results that may better reflect the situation *in vivo* [25]. In contrast, using succinate (without rotenone) leads to mitochondrial inhibition by oxaloacetate and yields results contrasting the *in vivo* results [25].

Enhanced ROS production in mtDNA mutator mitochondria under conditions of ADP-stimulated oxidative phosphorylation. Mitochondria in healthy active cells would always be in some degree of state 3 (active oxidative phosphorylation), although they may not always be fully activated in this respect. To more closely resemble the conditions *in vivo*, we therefore studied mitochondrial ROS production (and respiratory activity) in wildtype and mtDNA mutator mice mitochondria in the presence of high levels of ADP.

As expected, respiratory activity was increased (Fig. 6a, thin blue line), whereas ROS production (Fig. 6a, heavy blue line) was reduced in wildtype heart mitochondria stimulated by ADP, in agreement with [61]. This ROS-attenuating effect of ADP was clearly less pronounced in mtDNA mutator mitochondria (Fig. 6a, heavy red line) than in wildtype mitochondria. The rate of ROS production after the addition of ADP was thus higher in the mtDNA mutator mouse mitochondria than in wildtype mitochondria supported by palmitoyl-CoA + carnitine (Fig. 6a).

The rate of oxygen consumption in state 3 (after ADP addition) was not different between mitochondria from wildtype and mtDNA mutator mice when palmitoyl-CoA was used as substrate (in agreement with [23]) but with other substrates, the rate in the mutator mitochondria was generally lower (in agreement with [28]) (Fig. 6b; Fig. S1 in the Online Resource 1).

Similarly, to what is shown here for palmitoyl-CoA + + carnitine, the presence of ADP reduced ROS production with other substrates – with the most pronounced effect seen with succinate (without rotenone) (Fig. 6c). Notably, in the presence of ADP (state 3), a higher rate of ROS production in mutator versus wildtype mitochondria was evident in mitochondria energized not only by palmitoyl-CoA + carnitine but also in mitochondria energized by pyruvate + malate; the ROS production rate was equal on succinate without rotenone (Fig. 6c; Fig. S1 in the Online Resource 1).

To confirm these important observations obtained in the Oroboros system, we also examined ROS production in a plate-reader system. Also, here, mtDNA mutator heart mitochondria showed higher rates of ROS production with all three types of substrates tested (Fig. 6d). Remarkably, under these physiologically relevant conditions of ADP-stimulated oxidative phosphorylation, even succinate without rotenone tended to show enhanced ROS production in mutant mitochondria compared to wildtype mitochondria (Fig. 6c), in clear contrast to the outcome without ADP and rotenone (Fig. 1). Thus, the very high ROS production rate via reverse electron flux with succinate (without rotenone) was drastically reduced in the presence of ADP (Fig. 6d).

Thus, under the most relevant physiological conditions (active oxidative phosphorylation), mtDNA mutator mitochondria produce more ROS than wildtype mitochondria. The ROS production measured under these conditions is thus in accordance with the results of the measurements *in vivo* [25].

Increased oxidative stress in liver from mtDNA mutator *in vivo*. As mitochondria from mtDNA mutator mice showed enhanced ROS production under physiological conditions, we examined if this is associated with an actual increase in oxidative stress in mtDNA mutator mouse tissues. Therefore, we measured levels of 4-hydroxynonenal adducts (HNE-adducts), a marker of oxidative modification originating from lipid peroxidation of proteins, in liver extracts (Fig. 7, a-c). We detected both clear increases in the level of adducts of specific molecular weights (specific proteins) (see e.g., band at ≈28 kDa in Fig. 7a) and a general increase in the level of adduct formation (Fig. 7, b and c) in whole liver lysate of mtDNA mutator mice (Fig. 7, a-c).

In addition to measuring 4-HNE-adducts, we also examined the formation of protein carbonyls, generally used as a marker of oxidative stress [62]. Higher levels of carbonyl groups were observed in lysates from livers from mtDNA mutator mice as compared to wildtype mice (Fig. 7, d and e), as expected both from the 4-HNE-adduct data above and from earlier studies [20].

We therefore conclude that at least in certain tissues, an increased rate of mitochondrial mutations may result in an increase in oxidative damage, probably mediated via an increased ROS production.

DISCUSSION

According to the mitochondrial hypothesis of aging [2, 3], aging is caused by mutations in mitochondrial DNA that would lead to alterations in the mitochondrially encoded proteins in the respiratory chain. This would lead to increases in mitochondrial ROS production. This would then constitute a vicious cycle where the ROS thus produced would lead to further mitochondrial mutations and thus further alterations in the respiratory chain, leading to general oxidative damage: aging.

However, clearly one prediction of the hypothesis is that mitochondria with increased levels of mutations in their DNA should produce enhanced amounts of ROS. Until now this has not been demonstrated to

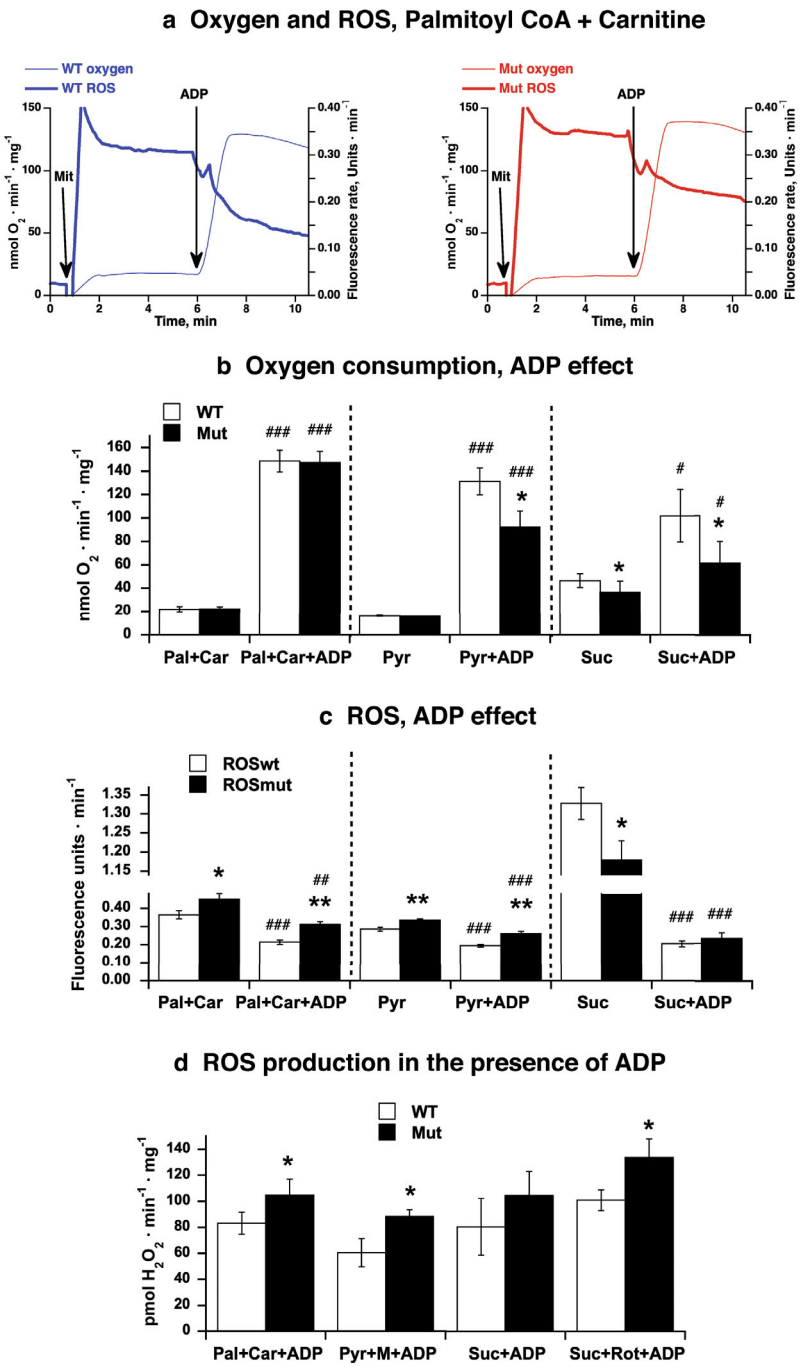

Fig. 6. ROS production in mitochondria stimulated by ADP. a) Representative traces of simultaneously measured oxygen consumption (*thin lines*) and Amplex Red fluorescence (*thick lines*) in wildtype (*blue lines*) and mtDNA mutator (*red lines*) heart mitochondria energized by palmitoyl-CoA + carnitine and then stimulated with ADP. Additions were 0.2 mg/ml mitochondria (Mit), and 450 µM ADP. Simultaneous measurement of oxygen and fluorescence was done by O2k-Fluorescence Module. b) Oxygen consumption rates in wildtype and mtDNA mutator mitochondria supported by palmitoyl-CoA + carnitine (Pal + Car) or pyruvate + malate (Pyr+ M) or succinate (Suc) as in (a); the effect of ADP addition. The values represent means ± SE of 5-7 independent mitochondrial preparations for each genotype. * Statistically significant difference between wildtype and mtDNA mutator mitochondria ($p < 0.05$). #, ### Indicates significant effects of ADP ($p < 0.05$ and $p < 0.001$). c) Rates of ROS production measured simultaneously with oxygen consumption in wildtype and mtDNA mutator mitochondria supported by palmitoyl-CoA + carnitine (Pal + Car) or pyruvate + malate (Pyr+ M) or succinate (Suc) as in (a); the effect of ADP addition. The values represent means ± SE of 5-7 independent mitochondrial preparations for each genotype. *, ** Statistically significant difference between wildtype and mtDNA mutator mitochondria ($p < 0.05$ and $p < 0.01$). ##, ### Indicates significant effects of ADP ($p < 0.01$ and $p < 0.001$). d) Rates of ROS production under conditions of active oxidative phosphorylation. ROS production was measured using a plate-reader simultaneously for all substrates including succinate in the presence of rotenone. 450 µM ADP was present before addition of mitochondria. The values represent means ± SE of 3 independent mitochondrial preparations. * Statistically significant difference between wildtype and mtDNA mutator mitochondria ($p < 0.05$).

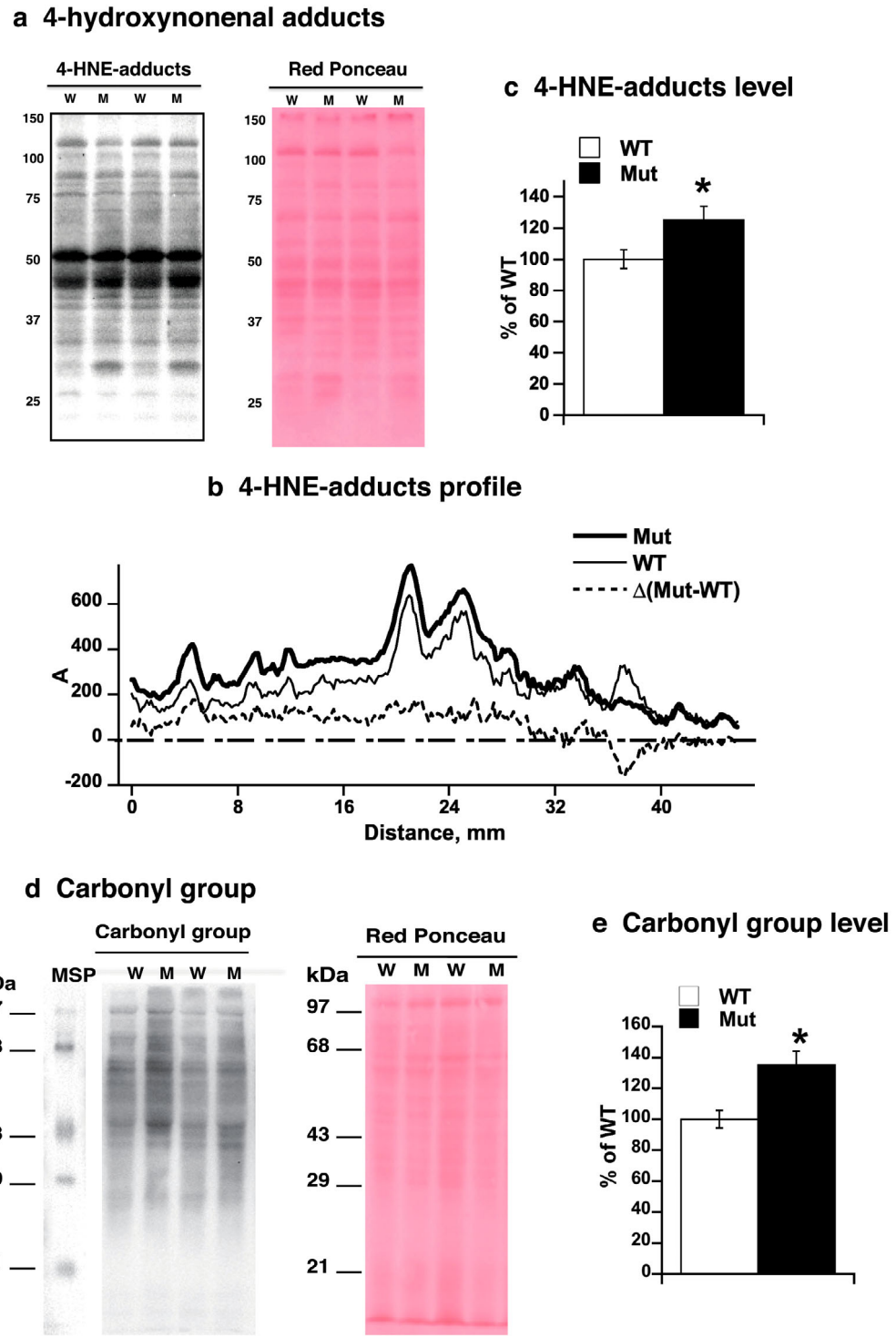

Fig. 7. Oxidative damage in wildtype and mtDNA mutator mitochondria. a) Representative immunoblot analysis of 4-hydroxy-nonenal (4-HNE) adducts and corresponding Red Ponceau staining in liver whole tissue lysate from mtDNA mutator (M) and wildtype mice (W) (15 μg protein/lane). b) Profile of 4-HNE-adducts in liver lysate. Lines indicate mean profiles of adducts examined in single or duplicate lanes as in figure (a) (*heavy* line for mtDNA mutator liver, $n = 7$; *thin* line for wildtype liver, $n = 5$). *Dashed* line was obtained by subtraction of wildtype mean profile from mtDNA mutator mean profile. c) Relative 4-HNE-adducts amounts in muscle and liver lysate. Western blots as in (a) were quantified and the total area under the curve was measured. The mean total amount of 4-HNE adducts in wildtype tissue was set to 100% and the levels of 4-HNE-adducts in mtDNA mutator tissue is expressed relative to this. The values represent the means ± SE of 5-7 independent tissue preparations from wildtype and mtDNA mutator mice. d) Representative immunoblot of carbonylated proteins and corresponding Red Ponceau staining of membrane in liver lysate. MSP, Mixture of Standard Proteins with attached DNP-residues. e) Relative carbonylation in liver lysate. Western blots as in (d) were analyzed principally as in (c); $n = 3$. * Indicates statistically significant difference between wildtype and mtDNA mutator mice ($p < 0.05$).

be the case, rather the opposite [20, 23, 24]. Due to the importance of understanding the nature of aging, we have here reexamined the effects of enhanced mitochondrial mutation rates on mitochondrial ROS production. We find that the lowered rate of ROS production earlier observed in the mtDNA mutator mice was due to the traditional, succinate-based experimental design used for the determination of ROS production. We demonstrate here that when experimental conditions are used that more closely approach physiologically relevant conditions, an enhanced level of ROS production is indeed observed in the mitochondria of the mtDNA mutator mice. Whereas these findings do not prove that the manifestations of aging are caused by increased ROS production due to increased mitochondrial mutations, they do reawaken this hypothesis and thus open for further investigations into the enigma of aging.

Observations of diminished ROS production in mtDNA mutator mitochondria are caused by the traditional experimental design. Earlier [23, 24], as well as present observations (Fig. 1) have consistently found reduced ROS production in mtDNA mutator mitochondria under the conditions traditionally utilized for measuring mitochondrial ROS production. We have here in detail analyzed the cause for this low ROS production rate.

We found that when wildtype mitochondria were oxidizing succinate under conditions when the oxidation was not inhibited by oxaloacetate accumulation, the mitochondria displayed ordinary respiratory control, i.e., respiration was stimulated by ADP and FCCP. Under these conditions, a high membrane potential was reached in the basal state (207 mV). As expected, when mtDNA mutator mice mitochondria were examined under the same conditions, the respiratory capacity was more than halved, leading to a slightly lower membrane potential (199 mV). In these mitochondria, the rate of ROS production in the presence of ADP was actually slightly higher in the mtDNA mutator mice mitochondria, in agreement with expectations that the mutations in the mitochondrial genome resulted in malfunctions in the respiratory chain components.

However, when the mitochondria were examined as is traditionally done in ROS investigations, i.e., in the absence of rotenone, the accumulation of oxaloacetate led to a strong inhibition of the succinate oxidation system. The respiratory rate was no longer determined by the membrane potential, it is e.g., not stimulated with FCCP, but it was limited by the low (inhibited) activity of the succinate dehydrogenase. Nonetheless, the respiration could raise the membrane potential to 206 mV. This membrane potential is sufficient to drive the electrons up to Complex I, and a high rate of ROS production occurred from this site. In the mtDNA mutator mitochondria, the lowered capacity of the respiratory system meant that it could only drive the membrane potential up to 174 mV; this was insufficient to drive the electrons to Complex I with the same capacity. A lowered rate of ROS production was thus observed, as reverse electron transfer is very sensitive to the membrane potential (reviewed in [40, 41, 63], also verified in brown-fat mitochondria [32]). The reason for the lowered rate of ROS production seen in the mtDNA mutator mitochondria is thus the artificial situation, with a profoundly inhibited activity of succinate oxidation due to the accumulation of oxaloacetate, a situation that does not occur normally in respiring mitochondria; it may, however, occur in ischemia-reperfusion injury and succinate dehydrogenase deficiency [53, 54]. The concept that mtDNA mutator mitochondria display lower rates of ROS production in general is thus an extrapolation from observations performed under very special conditions.

Increased ROS production in mtDNA mutator mitochondria with physiologically relevant substrates and conditions. We find that, in contrast to what we observe for succinate-derived ROS production, ROS production derived from Complex I substrates, fatty acid substrates, and during active oxidative phosphorylation (with any substrate) was *increased* in mtDNA mutator mitochondria, compared to wildtype mitochondria. Higher ROS production in isolated mitochondria from mtDNA mutator mice is an important observation, implying that mitochondrial mutations can indeed increase oxidative damage under physiological conditions.

Divergent magnitudes of ROS production on Complex I- versus Complex II-linked substrates are not unique for the mtDNA mutator case described here. In entirely different types of studies, a lower ROS production from succinate but higher from Complex I substrates has been reported [64, 65]. In these studies, as in ours, the lowered rates were associated with a reduced membrane potential [64, 65].

ROS production supported by Complex I substrates in mtDNA mutator mice has earlier been investigated [19, 23, 24]. In contrast to our observations, in these studies, ROS production was not higher in mtDNA mutator mitochondria than in wildtype mitochondria. One reason for this discrepancy may be the use of homovanillic acid for detecting ROS [19, 24]. Indeed, very high rates of hydrogen peroxide release (≈ 3000 pmol/min/mg on pyruvate) were reported, values which are more than thirty times higher than our values (≈ 90 pmol/min/mg) and values reported elsewhere (reviewed in [66]). Those observations may therefore be ascribed to methodological differences. However, Kukat et al. [23] found no difference between wildtype and mtDNA mutator heart mitochondria despite using very similar methods to the present paper, but ROS production rate was also much higher in [23]

compared to what is observed in the present article. We have no explanation for these discrepancies.

Importantly we find that investigating ROS production during ongoing oxidative phosphorylation is an essential way to further approach physiological conditions.

Also during active oxidative phosphorylation, the ROS production in mtDNA mutator mitochondria is higher than in wildtype mitochondria. Mitochondria in normal cells are always at least to some degree in state 3 (active oxidative phosphorylation), and conditions where ROS production is studied in the presence of ADP should thus better reflect the situation *in vivo* [13, 45]. We found that during active oxidative phosphorylation, ROS production was higher in mtDNA mutator mitochondria than in wildtype mitochondria, and this was the case with all different substrates studied here (including succinate). This result principally agrees with the observed increased ROS production in mitochondrial state 3 (in the presence of ADP) from normally aged animals as compared with younger animals [13, 61].

A possible causative role of mitochondrial ROS for cellular oxidative damage. The contribution of ROS production to the aging process is a debated topic [4, 67]. ROS can cause damage to proteins, lipids, and DNA in the cell, but its role in the aging process is unclear. Mitochondria are the most important source of ROS in the cell. It has been estimated that ≈0.4% of oxygen consumed is converted to ROS during mitochondrial respiration [40]. However, the level of ROS is not determined solely by the production rate but also by the effects of e.g., antioxidants. Still, we find that the lipid peroxidation rate in liver homogenates was enhanced in mtDNA mutator mice (Fig. S2 in the Online Resource 1), in parallel to the increase in mitochondrial ROS production generally described above in mtDNA mutator mice. Accordingly, we found evidence for increased oxidative damage in liver lysates from the mtDNA mutator mice, in agreement with [20]. The observed increases in 4-HNE adducts and protein carbonyl groups are likely important indicators of the pathology of mtDNA mutator mice. To what degree this reflects what occurs during normal aging can of course not be deduced from these observations in themselves, but our results indicate that mutations in the mitochondria may result in higher ROS production and higher ROS levels that in their turn could induce further mitochondrial mutations and thus enhanced ROS production in a self-reinforcing scheme.

CONCLUSIONS

This paper demonstrates that in contrast to what has earlier been concluded from studies using a traditional experimental design for measuring ROS production, the capacity for ROS production is increased in mtDNA mutator mice when studies are performed under conditions more closely approaching physiological conditions. These enhanced rates of ROS production in mtDNA mutator mice are associated with increased signs of oxidative damage in tissues of mtDNA mutator mice. The present studies are thus compatible with hypotheses that suggest that increased levels of mitochondrial mutations lead to enhanced rates of ROS production and elevated oxidative damage of tissues, and thus that aging processes may be understandable as being the results of enhanced levels of mitochondrial DNA mutations.

Supplementary information. The online version contains supplementary material available at https://doi.org/10.1134/S0006297924020081.

Acknowledgments. The authors thank Aleksandra Trifunovic for providing the initial breeding pair of mtDNA mutator mice, Vladimir Skulachev for stimulating discussions, Anton A. Tonshin for technical assistance, and Sofie Wagenius for establishing and verifying mouse strains.

Contributions. BC, JN, and IGS conceived and designed the work; experiments were performed by DE and IGS (oxygen consumption and ROS), NG (oxidative stress biomarkers), AVK and MYV (ROS), NP (immunoblotting), IGS (isolation of mitochondria and membrane potential); MYV, NG, and IGS analyzed results; DE, IGS, and JN wrote the manuscript. All authors revised the manuscript and approved the final version.

Funding. This study was supported by grants from the Swedish Research Council. AVK was supported by a salary from the Academic Initiative of Stockholm University.

Ethics declarations. The experiments were approved by the Animal Ethics Committee of the North Stockholm region.

Conflict of interest. The authors of this work declare that they have no conflicts of interest.

REFERENCES

1. Sanchez-Contreras, M., and Kennedy, S. R. (2022) The complicated nature of somatic mtDNA mutations in aging, *Front. Aging*, **2**, 805126, doi: 10.3389/fragi.2021.805126.
2. Harman, D. (2003) The free radical theory of aging, *Antioxid. Redox Signal.*, **5**, 557-561, doi: 10.1089/152308603770310202.
3. Skulachev, V. P., and Lyamzaev, K. G. (2021) *Mitochondrial Reactive Oxygen Species Aging Theory*, in Encyclopedia of Gerontology and Population Aging (Gu, D., and Dupre, M. E., eds) Springer International Publishing, Cham, 2021, pp. 3249-3256, doi: 10.1007/978-3-030-22009-9_47.

4. Salmon, A. B., Richardson, A., and Perez, V. I. (2010) Update on the oxidative stress theory of aging: does oxidative stress play a role in aging or healthy aging?, *Free Radic. Biol. Med.*, **48**, 642-655, doi: 10.1016/j.freeradbiomed.2009.12.015.
5. Lagouge, M., and Larsson, N. G. (2013) The role of mitochondrial DNA mutations and free radicals in disease and ageing, *J. Intern. Med.*, **273**, 529-543, doi: 10.1111/joim.12055.
6. Brand, M. D. (2020) Riding the tiger – physiological and pathological effects of superoxide and hydrogen peroxide generated in the mitochondrial matrix, *Crit. Rev. Biochem. Mol. Biol.*, **55**, 592-661, doi: 10.1080/10409238.2020.1828258.
7. Edgar, D., and Trifunovic, A. (2009) The mtDNA mutator mouse: Dissecting mitochondrial involvement in aging, *Aging (Albany NY)*, **1**, 1028-1032, doi: 10.18632/aging.100109.
8. Larsson, N. G. (2010) Somatic mitochondrial DNA mutations in mammalian aging, *Annu. Rev. Biochem.*, **79**, 683-706, doi: 10.1146/annurev-biochem-060408-093701.
9. Capel, F., Rimbert, V., Lioger, D., Diot, A., Rousset, P., Mirand, P. P., Boirie, Y., Morio, B., and Mosoni, L. (2005) Due to reverse electron transfer, mitochondrial H_2O_2 release increases with age in human vastus lateralis muscle although oxidative capacity is preserved, *Mech. Ageing Dev.*, **126**, 505-511, doi: 10.1016/j.mad.2004.11.001.
10. Sohal, R. S., Arnold, L. A., and Sohal, B. H. (1990) Age-related changes in antioxidant enzymes and prooxidant generation in tissues of the rat with special reference to parameters in two insect species, *Free Radic. Biol. Med.*, **9**, 495-500, doi: 10.1016/0891-5849(90)90127-5.
11. Lass, A., Sohal, B. H., Weindruch, R., Forster, M. J., and Sohal, R. S. (1998) Caloric restriction prevents age-associated accrual of oxidative damage to mouse skeletal muscle mitochondria, *Free Radic. Biol. Med.*, **25**, 1089-1097, doi: 10.1016/S0891-5849(98)00144-0.
12. Mansouri, A., Muller, F. L., Liu, Y., Ng, R., Faulkner, J., Hamilton, M., Richardson, A., Huang, T. T., Epstein, C. J., and Van Remmen, H. (2006) Alterations in mitochondrial function, hydrogen peroxide release and oxidative damage in mouse hind-limb skeletal muscle during aging, *Mech. Ageing Dev.*, **127**, 298-306, doi: 10.1016/j.mad.2005.11.004.
13. Chabi, B., Ljubicic, V., Menzies, K. J., Huang, J. H., Saleem, A., and Hood, D. A. (2008) Mitochondrial function and apoptotic susceptibility in aging skeletal muscle, *Aging Cell*, **7**, 2-12, doi: 10.1111/j.1474-9726.2007.00347.x.
14. Hansford, R. G., Hogue, B. A., and Mildaziene, V. (1997) Dependence of H2O2 formation by rat heart mitochondria on substrate availability and donor age, *J. Bioenerg. Biomembr.*, **29**, 89-95, doi: 10.1023/A:1022420007908.
15. Drew, B., Phaneuf, S., Dirks, A., Selman, C., Gredilla, R., Lezza, A., Barja, G., and Leeuwenburgh, C. (2003) Effects of aging and caloric restriction on mitochondrial energy production in gastrocnemius muscle and heart, *Am. J. Physiol. Regul. Integr. Comp. Physiol.*, **284**, R474-R480, doi: 10.1152/ajpregu.00455.2002.
16. Simmons, R. A., Suponitsky-Kroyter, I., and Selak, M. A. (2005) Progressive accumulation of mitochondrial DNA mutations and decline in mitochondrial function lead to beta-cell failure, *J. Biol. Chem.*, **280**, 28785-28791, doi: 10.1074/jbc.M505695200.
17. Papa, S., Sardanelli, A. M., Capitanio, N., and Piccoli, C. (2009) Mitochondrial respiratory dysfunction and mutations in mitochondrial DNA in PINK1 familial parkinsonism, *J. Bioenerg. Biomemb.*, **41**, 509-516, doi: 10.1007/s10863-009-9252-4.
18. Trifunovic, A., Wredenberg, A., Falkenberg, M., Spelbrink, J. N., Rovio, A. T., Bruder, C. E., Bohlooly, Y. M., Gidlof, S., Oldfors, A., Wibom, R., Tornell, J., Jacobs, H. T., and Larsson, N. G. (2004) Premature ageing in mice expressing defective mitochondrial DNA polymerase, *Nature*, **429**, 417-423, doi: 10.1038/nature02517.
19. Kujoth, G. C., Hiona, A., Pugh, T. D., Someya, S., Panzer, K., Wohlgemuth, S. E., Hofer, T., Seo, A. Y., Sullivan, R., Jobling, W. A., Morrow, J. D., Van Remmen, H., Sedivy, J. M., Yamasoba, T., Tanokura, M., Weindruch, R., Leeuwenburgh, C., and Prolla, T. A. (2005) Mitochondrial DNA mutations, oxidative stress, and apoptosis in mammalian aging, *Science*, **309**, 481-484, doi: 10.1126/science.1112125.
20. Trifunovic, A., Hansson, A., Wredenberg, A., Rovio, A. T., Dufour, E., Khvorostov, I., Spelbrink, J. N., Wibom, R., Jacobs, H. T., and Larsson, N. G. (2005) Somatic mtDNA mutations cause aging phenotypes without affecting reactive oxygen species production, *Proc. Natl. Acad. Sci. USA*, **102**, 17993-17998, doi: 10.1073/pnas.0508886102.
21. Kolesar, J. E., Safdar, A., Abadi, A., MacNeil, L. G., Crane, J. D., Tarnopolsky, M. A., and Kaufman, B. A. (2014) Defects in mitochondrial DNA replication and oxidative damage in muscle of mtDNA mutator mice, *Free Radic. Biol. Med.*, **75**, 241-251, doi: 10.1016/j.freeradbiomed.2014.07.038.
22. Yu, T., Slone, J., Liu, W., Barnes, R., Opresko, P. L., Wark, L., Mai, S., Horvath, S., and Huang, T. (2022) Premature aging is associated with higher levels of 8-oxoguanine and increased DNA damage in the Polg mutator mouse, *Aging Cell*, **21**, e13669, doi: 10.1111/acel.13669.
23. Kukat, A., Dogan, S. A., Edgar, D., Mourier, A., Jacoby, C., Maiti, P., Mauer, J., Becker, C., Senft, K., Wibom, R., Kudin, A. P., Hultenby, K., Flogel, U., Rosenkranz, S., Ricquier, D., Kunz, W. S., and Trifunovic, A. (2014) Loss of UCP2 attenuates mitochondrial dysfunction without altering ROS production and uncou-

pling activity, *PLoS Genet.*, **10**, e1004385, doi: 10.1371/journal.pgen.1004385.

24. Hiona, A., Sanz, A., Kujoth, G. C., Pamplona, R., Seo, A. Y., Hofer, T., Someya, S., Miyakawa, T., Nakayama, C., Samhan-Arias, A. K., Servais, S., Barger, J. L., Portero-Otin, M., Tanokura, M., Prolla, T. A., and Leeuwenburgh, C. (2010) Mitochondrial DNA mutations induce mitochondrial dysfunction, apoptosis and sarcopenia in skeletal muscle of mitochondrial DNA mutator mice, *PLoS One*, **5**, e11468, doi: 10.1371/journal.pone.0011468.
25. Logan, A., Shabalina, I. G., Prime, T. A., Rogatti, S., Kalinovich, A. V., Hartley, R. C., Budd, R. C., Cannon, B., and Murphy, M. P. (2014) *In vivo* levels of mitochondrial hydrogen peroxide increase with age in mtDNA mutator mice, *Aging Cell*, **13**, 765-768, doi: 10.1111/acel.12212.
26. Shabalina, I. G., Vyssokikh, M. Y., Gibanova, N., Csikasz, R. I., Edgar, D., Hallden-Waldemarson, A., Rozhdestvenskaya, Z., Bakeeva, L. E., Vays, V. B., Pustovidko, A. V., Skulachev, M. V., Cannon, B., Skulachev, V. P., and Nedergaard, J. (2017) Improved health-span and lifespan in mtDNA mutator mice treated with the mitochondrially targeted antioxidant SkQ1, *Aging*, **9**, 315-339, doi: 10.18632/aging.101174.
27. Dai, D. F., Chen, T., Wanagat, J., Laflamme, M., Marcinek, D. J., Emond, M. J., Ngo, C. P., Prolla, T. A., and Rabinovitch, P. S. (2010) Age-dependent cardiomyopathy in mitochondrial mutator mice is attenuated by overexpression of catalase targeted to mitochondria, *Aging Cell*, **9**, 536-544, doi: 10.1111/j.1474-9726.2010.00581.x.
28. Edgar, D., Shabalina, I., Camara, Y., Wredenberg, A., Calvaruso, M. A., Nijtmans, L., Nedergaard, J., Cannon, B., Larsson, N. G., and Trifunovic, A. (2009) Random point mutations with major effects on protein-coding genes are the driving force behind premature aging in mtDNA mutator mice, *Cell Metab.*, **10**, 131-138, doi: 10.1016/j.cmet.2009.06.010.
29. Silva, J. P., Shabalina, I. G., Dufour, E., Petrovic, N., Backlund, E. C., Hultenby, K., Wibom, R., Nedergaard, J., Cannon, B., and Larsson, N. G. (2005) SOD2 overexpression: enhanced mitochondrial tolerance but absence of effect on UCP activity, *EMBO J.*, **24**, 4061-4070, doi: 10.1038/sj.emboj.7600866.
30. Udenfriend, S., Stein, S., Bohlen, P., Dairman, W., Leimgruber, W., and Weigele, M. (1972) Fluorescamine: a reagent for assay of amino acids, peptides, proteins, and primary amines in the picomole range, *Science*, **178**, 871-872, doi: 10.1126/science.178.4063.871.
31. Kettle, A. J., Carr, A. C., and Winterbourn, C. C. (1994) Assays using horseradish peroxidase and phenolic substrates require superoxide dismutase for accurate determination of hydrogen peroxide production by neutrophils, *Free Radic. Biol. Med.*, **17**, 161-164, doi: 10.1016/0891-5849(94)90111-2.
32. Shabalina, I. G., Vrbacky, M., Pecinova, A., Kalinovich, A. V., Drahota, Z., Houstek, J., Mracek, T., Cannon, B., and Nedergaard, J. (2014) ROS production in brown adipose tissue mitochondria: The question of UCP1-dependence, *Biochim. Biophys. Acta*, **1837**, 2017-2030, doi: 10.1016/j.bbabio.2014.04.005.
33. Salvi, M., Battaglia, V., Brunati, A. M., La Rocca, N., Tibaldi, E., Pietrangeli, P., Marcocci, L., Mondovi, B., Rossi, C. A., and Toninello, A. (2007) Catalase takes part in rat liver mitochondria oxidative stress defense, *J. Biol. Chem.*, **282**, 24407-24415, doi: 10.1074/jbc.M701589200.
34. Panov, A., Dikalov, S., Shalbuyeva, N., Hemendinger, R., Greenamyre, J. T., and Rosenfeld, J. (2007) Species- and tissue-specific relationships between mitochondrial permeability transition and generation of ROS in brain and liver mitochondria of rats and mice, *Am. J. Physiol. Cell Physiol.*, **292**, C708-C718, doi: 10.1152/ajpcell.00202.2006.
35. Shabalina, I. G., Hoeks, J., Kramarova, T. V., Schrauwen, P., Cannon, B., and Nedergaard, J. (2010) Cold tolerance of UCP1-ablated mice: A skeletal muscle mitochondria switch toward lipid oxidation with marked UCP3 up-regulation not associated with increased basal, fatty acid- or ROS-induced uncoupling or enhanced GDP effects, *Biochim. Biophys. Acta*, **1797**, 968-980, doi: 10.1016/j.bbabio.2010.02.033.
36. Nedergaard, J. (1983) The relationship between extramitochondrial Ca^{2+} concentration, respiratory rate, and membrane potential in mitochondria from brown adipose tissue of the rat, *Eur. J. Biochem.*, **133**, 185-191, doi: 10.1111/j.1432-1033.1983.tb07446.x.
37. Sahlin, K., Shabalina, I. G., Mattsson, C. M., Bakkman, L., Fernstrom, M., Rozhdestvenskaya, Z., Enqvist, J. K., Nedergaard, J., Ekblom, B., and Tonkonogi, M. (2010) Ultraendurance exercise increases the production of reactive oxygen species in isolated mitochondria from human skeletal muscle, *J. Appl. Physiol.*, **108**, 780-787, doi: 10.1152/japplphysiol.00966.2009.
38. Shabalina, I. G., Petrovic, N., Kramarova, T. V., Hoeks, J., Cannon, B., and Nedergaard, J. (2006) UCP1 and defense against oxidative stress. 4-Hydroxy-2-nonenal effects on brown fat mitochondria are uncoupling protein 1-independent, *J. Biol. Chem.*, **281**, 13882-13893, doi: 10.1074/jbc.M601387200.
39. Skulachev, V. P. (1996) Role of uncoupled and non-coupled oxidations in maintenance of safely low levels of oxygen and its one-electron reductants, *Q. Rev. Biophys.*, **29**, 169-202, doi: 10.1017/S0033583500005795.
40. Murphy, M. P. (2009) How mitochondria produce reactive oxygen species, *Biochem. J.*, **417**, 1-13, doi: 10.1042/BJ20081386.
41. Brand, M. D. (2010) The sites and topology of mitochondrial superoxide production, *Exp. Gerontol.*, **45**, 466-472, doi: 10.1016/j.exger.2010.01.003.
42. Lambert, A. J., Boysen, H. M., Buckingham, J. A., Yang, T., Podlutsky, A., Austad, S. N., Kunz, T. H.,

Buffenstein, R., and Brand, M. D. (2007) Low rates of hydrogen peroxide production by isolated heart mitochondria associate with long maximum lifespan in vertebrate homeotherms, *Aging Cell*, **6**, 607-618, doi: 10.1111/j.1474-9726.2007.00312.x.

43. Scialo, F., Sriram, A., Fernandez-Ayala, D., Gubina, N., Lohmus, M., Nelson, G., Logan, A., Cooper, H. M., Navas, P., Enriquez, J. A., Murphy, M. P., and Sanz, A. (2016) Mitochondrial ROS produced via reverse electron transport extend animal lifespan, *Cell Metab.*, **23**, 725-734, doi: 10.1016/j.cmet.2016.03.009.
44. Brand, M. D., Goncalves, R. L. S., Orr, A. L., Vargas, L., Gerencser, A. A., Borch Jensen, M., Wang, Y. T., Melov, S., Turk, C. N., Matzen, J. T., Dardov, V. J., Petrassi, H. M., Meeusen, S. L., Perevoshchikova, I. V., Jasper, H., Brookes, P. S., and Ainscow, E. K. (2016) Suppressors of superoxide-H_2O_2 production at site IQ of mitochondrial complex I protect against stem cell hyperplasia and ischemia-reperfusion injury, *Cell Metab.*, **24**, 582-592, doi: 10.1016/j.cmet.2016.08.012.
45. Goncalves, R. L. S., Quinlan, C. L., Perevoshchikova, I. V., Hey-Mogensen, M., and Brand, M. D. (2015) Sites of superoxide and hydrogen peroxide production by muscle mitochondria assessed *ex vivo* under conditions mimicking rest and exercise, *J. Biol. Chem.*, **290**, 209-227, doi: 10.1074/jbc.M114.619072.
46. Fendel, U., Tocilescu, M. A., Kerscher, S., and Brandt, U. (2008) Exploring the inhibitor binding pocket of respiratory complex I, *Biochim. Biophys. Acta*, **1777**, 660-665, doi: 10.1016/j.bbabio.2008.04.033.
47. Boveris, A., and Chance, B. (1973) The mitochondrial generation of hydrogen peroxide. General properties and effect of hyperbaric oxygen, *Biochem. J.*, **134**, 707-716, doi: 10.1042/bj1340707.
48. Korshunov, S. S., Skulachev, V. P., and Starkov, A. A. (1997) High protonic potential actuates a mechanism of production of reactive oxygen species in mitochondria, *FEBS Lett.*, **416**, 15-18, doi: 10.1016/S0014-5793(97)01159-9.
49. Fink, B. D., Bai, F., Yu, L., Sheldon, R. D., Sharma, A., Taylor, E. B., and Sivitz, W. I. (2018) Oxaloacetic acid mediates ADP-dependent inhibition of mitochondrial complex II-driven respiration, *J. Biol. Chem.*, **293**, 19932-19941, doi: 10.1074/jbc.RA118.005144.
50. Zeyelmaker, W. P., and Slater, E. C. (1967) The inhibition of succinate dehydrogenase by oxaloacetate, *Biochim. Biophys. Acta*, **132**, 210-212, doi: 10.1016/0005-2744(67)90214-8.
51. Nicholls, D. G. (1974) The influence of respiration and ATP hydrolysis on the proton-electrochemical gradient across the inner membrane of rat-liver mitochondria as determined by ion distribution, *Eur. J. Biochem.*, **50**, 305-315, doi: 10.1111/j.1432-1033.1974.tb03899.x.
52. Nicholls, D. G. (1977) The effective proton conduction of the inner membrane of mitochondria from brown adipose tissue. Dependency on proton electrochemical potential gradient, *Eur. J. Biochem.*, **77**, 349-356, doi: 10.1111/j.1432-1033.1977.tb11674.x.
53. Chouchani, E. T., Pell, V. R., Gaude, E., Aksentijevic, D., Sundier, S. Y., Robb, E. L., Logan, A., Nadtochiy, S. M., Ord, E. N., Smith, A. C., Eyassu, F., Shirley, R., Hu, C. H., Dare, A. J., James, A. M., Rogatti, S., Hartley, R. C., Eaton, S., Costa, A. S., Brookes, P. S., Davidson, S. M., Duchen, M. R., Saeb-Parsy, K., Shattock, M. J., Robinson, A. J., Work, L. M., Frezza, C., Krieg, T., and Murphy, M. P. (2014) Ischaemic accumulation of succinate controls reperfusion injury through mitochondrial ROS, *Nature*, **515**, 431-435, doi: 10.1038/nature13909.
54. Brockmann, K., Bjornstad, A., Dechent, P., Korenke, C. G., Smeitink, J., Trijbels, J. M., Athanassopoulos, S., Villagran, R., Skjeldal, O. H., Wilichowski, E., Frahm, J., and Hanefeld, F. (2002) Succinate in dystrophic white matter: a proton magnetic resonance spectroscopy finding characteristic for complex II deficiency, *Ann. Neurol.*, **52**, 38-46, doi: 10.1002/ana.10232.
55. Mills, E. L., Kelly, B., Logan, A., Costa, A. S., Varma, M., Bryant, C. E., Tourlomousis, P., Dabritz, J. H., Gottlieb, E., Latorre, I., Corr, S. C., McManus, G., Ryan, D., Jacobs, H. T., Szibor, M., Xavier, R. J., Braun, T., Frezza, C., Murphy, M. P., and O'Neill, L. A. (2016) Succinate dehydrogenase supports metabolic repurposing of mitochondria to drive inflammatory macrophages, *Cell*, **167**, 457-470.e413, doi: 10.1016/j.cell.2016.08.064.
56. Starkov, A. A., Fiskum, G., Chinopoulos, C., Lorenzo, B. J., Browne, S. E., Patel, M. S., and Beal, M. F. (2004) Mitochondrial alpha-ketoglutarate dehydrogenase complex generates reactive oxygen species, *J. Neurosci.*, **24**, 7779-7788, doi: 10.1523/JNEUROSCI.1899-04.2004.
57. Lambert, A. J., Buckingham, J. A., Boysen, H. M., and Brand, M. D. (2010) Low complex I content explains the low hydrogen peroxide production rate of heart mitochondria from the long-lived pigeon, *Columba livia*, *Aging Cell*, **9**, 78-91, doi: 10.1111/j.1474-9726.2009.00538.x.
58. Lesnefsky, E. J., Chen, Q., and Hoppel, C. L. (2016) Mitochondrial metabolism in aging heart, *Circ. Res.*, **118**, 1593-1611, doi: 10.1161/CIRCRESAHA.116.307505.
59. Perevoshchikova, I. V., Quinlan, C. L., Orr, A. L., Gerencser, A. A., and Brand, M. D. (2013) Sites of superoxide and hydrogen peroxide production during fatty acid oxidation in rat skeletal muscle mitochondria, *Free Radic. Biol. Med.*, **61**, 298-309, doi: 10.1016/j.freeradbiomed.2013.04.006.
60. Seifert, E. L., Estey, C., Xuan, J. Y., and Harper, M.-E. (2010) Electron transport chain-dependent and -independent mechanisms of mitochondrial H_2O_2 emission during long-chain fatty acid oxidation, *J. Biol. Chem.*, **285**, 5748-5758, doi: 10.1074/jbc.M109.026203.
61. Lopez-Torres, M., Gredilla, R., Sanz, A., and Barja, G. (2002) Influence of aging and long-term caloric

restriction on oxygen radical generation and oxidative DNA damage in rat liver mitochondria, *Free Radic. Biol. Med.*, **32**, 882-889, doi: 10.1016/S0891-5849(02)00773-6.

62. Dalle-Donne, I., Giustarini, D., Colombo, R., Rossi, R., and Milzani, A. (2003) Protein carbonylation in human diseases, *Trends Mol. Med.*, **9**, 169-176, doi: 10.1016/S1471-4914(03)00031-5.
63. Shabalina, I. G., and Nedergaard, J. (2011) Mitochondrial ('mild') uncoupling and ROS production: physiologically relevant or not?, *Biochem. Soc. Trans.*, **39**, 1305-1309, doi: 10.1042/BST0391305.
64. Bhattacharya, A., Lustgarten, M., Shi, Y., Liu, Y., Jang, Y. C., Pulliam, D., Jernigan, A. L., and Van Remmen, H. (2011) Increased mitochondrial matrix-directed superoxide production by fatty acid hydroperoxides in skeletal muscle mitochondria, *Free Radic. Biol. Med.*, **50**, 592-601, doi: 10.1016/j.freeradbiomed.2010.12.014.
65. Iacono, L. L., Boczkowski, J., Zini, R., Salouage, I., Berdeaux, A., Motterlini, R., and Morin, D. (2011) A carbon monoxide-releasing molecule (CORM-3) uncouples mitochondrial respiration and modulates the production of reactive oxygen species, *Free Radic. Biol. Med.*, **4**, 4, doi: 10.1016/j.freeradbiomed.2011.02.033.
66. Lambert, A. J., and Brand, M. D. (2009) Reactive oxygen species production by mitochondria, *Methods Mol. Biol.*, **554**, 165-181, doi: 10.1007/978-1-59745-521-3_11.
67. Perez, V. I., Bokov, A., Van Remmen, H., Mele, J., Ran, Q., Ikeno, Y., and Richardson, A. (2009) Is the oxidative stress theory of aging dead?, *Biochim. Biophys. Acta*, **1790**, 1005-1014, doi: 10.1016/j.bbagen.2009.06.003.